

Effect of Silicate on the Formation and Stability of Ni–Al LDH at the γ -Al₂O₃ Surface

Xiaoli Tan,^{†,‡} Ming Fang,[†] Xuemei Ren,[‡] Huiyang Mei,[‡] Dadong Shao,[‡] and Xiangke Wang^{*,†,‡,§}

[†]School of Environment and Chemical Engineering, North China Electric Power University, Beijing 102206, P.R. China

[‡]Institute of Plasma Physics, Chinese Academy of Sciences, P.O. Box 1126, Hefei, Anhui 230031, P.R. China

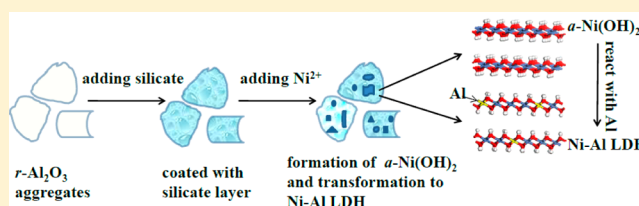
[#]Faculty of Engineering, King Abdulaziz University, Jeddah 21589, Saudi Arabia

[§]Collaborative Innovation Center of Radiation Medicine of Jiangsu Higher Education Institutions, Soochow University, Suzhou, Jiangsu 215123, P.R. China

S Supporting Information

ABSTRACT: The formation of mixed metal precipitates has been identified as a significant mechanism for the immobilization and elimination of heavy metal ions. Silicate is present in natural systems ubiquitously, which may interfere with metal uptake on the mineral surface and thereby influences the solubility of the precipitate. Herein, kinetic sorption and dissolution experiments combined with extended X-ray absorption fine structure spectroscopy (EXAFS) were

performed to elucidate the effect of silicate on the formation of Ni precipitates at the γ -Al₂O₃ surfaces. The uptake of Ni on γ -Al₂O₃ decreased with increasing amounts of silicate coated onto the γ -Al₂O₃ surface. Results of EXAFS analyses suggested the formation of Ni–Al layered double hydroxide (LDH) phases. The surface coating of silicate on γ -Al₂O₃ reduced Al release and finally resulted in a high Ni:Al ratio due to a lower extent of Al substitution into the precipitates. The presence of silicate prevented the growth of the precipitates and led to the formation of less stable Ni–Al LDH. The influence of silicate on the precipitate formation provided the evidence for the growth relationship between the precipitate and mineral substrate in the real environment. Increased rates of proton-promoted dissolution of Ni surface precipitates were mainly attributed to higher Ni:Al ratios in Ni–Al LDH precipitates formed in the presence of silicate.



INTRODUCTION

The mobility and bioavailability of heavy metals in aquatic and soil environments are often dictated by the sorption and desorption reactions occurring at the mineral/water interfaces.^{1–3} Formation of surface precipitates drastically reduces the free metal ion concentration in soil and sediment systems. The formation of mixed metal precipitates of Co(II), Zn(II), and Ni(II) has been identified on a range of clay mineral and metal oxide surfaces.^{1–6} Depending on the reaction conditions, either a metal hydroxide,⁷ a mixed layered double hydroxide (LDH),^{4–6,8} or a phyllosilicate^{9,10} may be formed at the mineral surface. Many research results have shown that the stability of the surface precipitates increases with increasing aging time,^{3,6,7} and this stabilization is attributed to the transformation of the metal hydroxide or LDH into a more stable phyllosilicate phase, with Ostwald ripening playing a more minor role.³ Thereby, identification of the possible type of precipitates on the mineral surface is important since this might lead to the long-term immobilization of potentially hazardous heavy metals in the contaminated soils and sediments in natural environment.

Most of the aforementioned literature focused on the simple mechanism of single-metal ion sorption on ideal mineral/water interfaces. It is not clearly understood as to how heavy metal

ions are sequestered in a natural environment since most realistic conditions contain multifactors (i.e., competitive metal ions or organic matters).^{6,11} Such competition is very important in the environment remediation; however, only a limited numbers of studies have addressed the similar research field as far as we know, such as the presence of interacting organic molecules or the metal ions and their influence on metal sequestration in precipitate phases.^{6,11,12} These studies suggested that the organic molecules influenced the formation of Ni–Al LDH.¹² Voegelin and Kretzschmar⁶ reported the formation of Zn–Ni LDH precipitates in the simultaneous presence of two metal cations (e.g., Ni and Zn) in soils. The Si element, the second most abundant element in nature,^{13–15} is easy to access in the water environment by dissolution of rock-forming silicates. Although it is present in the natural environment ubiquitously, the synergetic effect of silicate is seldom considered in the investigation of heavy metal ion sorption.^{16–20} As far as we know, only Schlegel and co-workers considered the impact of silicate on Zn sorption onto

Received: March 26, 2014

Revised: October 16, 2014

Accepted: October 23, 2014

Published: October 23, 2014

hectorite¹⁶ and montmorillonite.¹⁷ They showed the evidence for an epitaxial relationship between the precipitate and the mineral substrate. Considering the real environment sorption–desorption processes, it is of great importance to investigate the effect of silicate on heavy metal ions' precipitation–dissolution. Earlier studies on Ni precipitation proposed a model where silicate could migrate into the layers of Ni–Al LDH phases and helped to stabilize them.^{2,3,21} All these systems related the Si-containing minerals, and the precipitation formation or transformation may be dependent greatly on the structures of the substrates. Thereby, we herein addressed the presence of interacting silicates and their influence on Ni sequestration in the precipitate phases on γ -Al₂O₃. γ -Al₂O₃ was chosen as the Si-free adsorbent in order to clarify whether silicate was vital for the formation and stability of Ni surface precipitates, and the experimental evidence was sparse. The possible relationship between the Ni precipitation and the mineral substrates could be rightly enriched for this field.

With a small amount of silicate present, identification of Ni precipitate formation is challenging because of the limitations of current available data and spectroscopic signature. Herein, we systematically investigated the influence of silicate on the formation and stability of Ni precipitates on the γ -Al₂O₃ surface by a combined method of kinetic studies with extended X-ray absorption fine structure (EXAFS) spectroscopy. The Ni compounds were compared to model the formation of precipitates in the presence of silicate on γ -Al₂O₃. This study provided insight on the potential contribution of silicate on Ni precipitates and to evaluate the fate of Ni in the natural environment. The results were crucial to understand the physicochemical behaviors of Ni with metal oxides in the natural environment.

■ EXPERIMENTAL SECTION

Materials. γ -Al₂O₃ used in this work (Degussa, Aluminum Oxide C) has been previously used for Eu(III) sorption experiments.²² The N₂-BET specific surface area was measured to be 105 m²/g, and the point of zero charge (pHpzc) was calculated to be ~8.6 according to the method reported by Rabung et al.²³

Ni Sorption and Kinetics of Dissolution. Prior to initializing Ni sorption, the solids were hydrated for 24 h by suspending 3.0 g of γ -Al₂O₃ in 500 mL of 0.1 M NaNO₃ solution adjusted to pH 7.8 using 0.1 M HNO₃ or NaOH. After hydration of γ -Al₂O₃, Ni stock solution (0.01 M Ni(NO₃)₂) was added to achieve the initial concentrations of [Ni]_{initial} = 0.50 mM, [NaNO₃] = 0.01 M, and a solid/solution ratio = 3.0 g/L.

To assess the roles of silicate and γ -Al₂O₃ on Ni uptake, three experiments were performed by varying silicate concentrations. For the first (Al–HSiNi), a dilute γ -Al₂O₃ suspension (3.0 g/L) with a “high” solute silicate concentration ([Si]_{aq} = 0.50 mM Na₂SiO₃·H₂O) was prepared at pH 4.0. This suspension was allowed to react overnight without pH control before Ni addition. For the second (Al–LSiNi), a dilute γ -Al₂O₃ suspension (3.0 g/L) with a “low” solute silicate concentration ([Si]_{aq} = 0.05 mM Na₂SiO₃·H₂O) was prepared at pH 4.0, and the suspension was allowed to react overnight without pH control before Ni addition. For the third (Al–Ni), no silicate ([Si]_{aq} = 0 mM) in γ -Al₂O₃ suspension was prepared by mixing γ -Al₂O₃ stock suspension, NaNO₃ and Ni solution. In all experiments, pH was adjusted to 7.8 after Ni addition by adding negligible amounts of 0.01 or 0.1 mol/L HNO₃ or NaOH. After

given aging time ($0 \leq t \leq 312$ h), the suspension was pipetted from the reaction vessel with a pipet tip and then centrifuged to remove γ -Al₂O₃. Our pre-experiments suggested that 30 min at 9000 rpm was enough for the separation of solid from liquid phase. The separated liquid phases were analyzed for Ni, Si, and Al concentrations by inductively coupled plasma-atomic emission spectroscopy (ICP-AES) or atomic absorption spectrometry (AAS). The different addition sequences on the interaction of Ni(II) and silicate with γ -Al₂O₃ were studied as well. Detailed processes are shown in the Supporting Information.

The sorption of silicate on γ -Al₂O₃ (Al–HSi) was also carried out at pH 7.8 to examine the silicate sorption. The initial Ni concentration and silicate concentration at pH 7.8 were chosen to achieve high Ni loading on γ -Al₂O₃ while ensuring that the bulk solutions were undersaturated with respect to crystalline Ni(OH)₂(s) or Ni phyllosilicate(s).¹⁰ The theoretical solubility limit of Ni(OH)₂ in solution predicted from thermodynamic calculations were not particularly conclusive because the logK_{sp} (Ni(OH)₂) value reported in the literature varied over a wide range (–10.99 to –18.06).¹⁰ Complexation of Ni by dissolved silicate was not considered because no thermodynamic data were available. Therefore, the stability of the mixed Ni and Si solution (HSiNi) (pH 7.8, [Ni]_{initial} = 0.50 mM, [Si] = 0.50 mM, I = 0.1 M NaNO₃) used for the Al–HSiNi system was checked, and the concentrations were not changed.

Dissolution of the precipitates derived from the Al–HSiNi, Al–LSiNi, and Al–Ni systems was carried out by a replenishment technique as described by Scheckel and Sparks³ using HNO₃ (proton-promoted dissolution) at pH 4.0. From the aging Al–HSiNi, Al–LSiNi, and Al–Ni suspensions (aging time of 2 weeks), a 30 mL suspension (corresponding to 90 mg of solid) was withdrawn. After centrifugation, the supernatant was decanted, and 30 mL of the dissolution agent was added to the remaining solids. The suspensions were then placed on a reciprocating shaker at 20 °C for 24 h. The extraction steps were repeated 10 times (10 days) for the three samples. The ICP-AES or AAS was used to determine the concentrations of Ni, Si, and Al in the supernatants for Al–HSiNi, Al–LSiNi, and Al–Ni.

EXAFS Analysis. For EXAFS analysis, samples were examined *in situ* by centrifuging the suspensions, and the wet sorbent pastes were used for EXAFS spectra measurements. Nickel K-edge X-ray absorption spectra were recorded at the Shanghai Synchrotron Radiation Facility (SSRF, China) in fluorescence (for sorption samples) and in transmission (Ni(OH)₂, Ni–Al LDH, Ni phyllosilicate, silicated Ni–Al LDH, and Ni(OH)₂) modes. Detailed descriptions of EXAFS analysis are listed in the SI.

■ RESULTS AND DISCUSSION

Kinetics of Ni Sorption. The kinetics of Ni sorption and the impacts of silicate on Ni uptake onto γ -Al₂O₃ are shown in Figure 1A. No change in [Ni]_{aq} was observed in the HSiNi system, even after 312 h of reaction time (Figure 1A). The results indicated that Ni precipitates did not nucleate in solution or the nuclei were too small to be removed by centrifugation in the absence of γ -Al₂O₃. On the other hand, Ni sorption on the γ -Al₂O₃ surface was observed in Al–HSiNi, Al–LSiNi, and Al–Ni systems. For the Al–Ni system, Ni was adsorbed rapidly and amounted to 75% after contact time of 72 h. Then, the Ni sorption rate slowed down with increasing

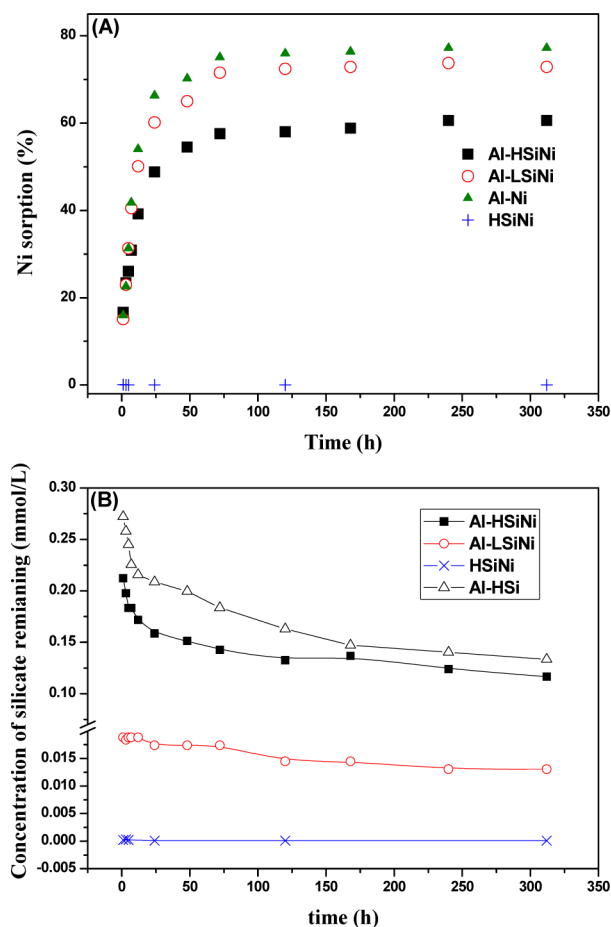


Figure 1. (A) Ni uptake as a function of contact time and silicate concentrations. (B) The uptake of silicate in the Al–HSiNi, Al–LSiNi, and Al–HSi systems. $[\gamma\text{-Al}_2\text{O}_3] = 3.0$ g/L, $[\text{Ni}]_{\text{initial}} = 0.5$ mM, $[\text{Si}]_{\text{initial}} = 0.5$ or 0.05 mM, $[\text{NaNO}_3] = 0.01$ M, and pH 7.8 for all experiments.

contact time, and $\sim 77\%$ of $[\text{Ni}]_{\text{initial}}$ was adsorbed after 312 h. For high silicate concentration (Al–HSiNi), the amount of Ni adsorbed on Al–HSiNi was relatively lower as compared to that of Ni adsorbed on Al–Ni. About 60% of $[\text{Ni}]_{\text{initial}}$ was adsorbed on the solid phase after the contact time of 312 h. For low silicate concentration (Al–LSiNi), the Ni sorption curve was between Al–HSiNi and Al–Ni systems. For the whole systems, the sorption of Ni on $\gamma\text{-Al}_2\text{O}_3$ was essentially completed in the first contact time of 72 h and then continued at much reduced rates. This continued sorption at a very low rate was attributed to the growth of precipitate phases.^{3,24} For the Al–HSiNi system, the amounts of Ni(II) retained for different addition sequences were discussed in the SI (Figure S1).

The kinetics of silicate sorption on $\gamma\text{-Al}_2\text{O}_3$ is shown in Figure 1B. In the absence of $\gamma\text{-Al}_2\text{O}_3$ (i.e., HSiNi), silicate remained constant in solution, which meant that the silicate did not form (co)precipitates with Ni. In the presence of $\gamma\text{-Al}_2\text{O}_3$ and high silicate concentration (Al–HSiNi), the uptake of silicate onto $\gamma\text{-Al}_2\text{O}_3$ occurred quickly, and the concentration of silicate was lowered from 0.5 mM to 0.22 mM in 24 h (about 56% of silicate was adsorbed onto $\gamma\text{-Al}_2\text{O}_3$) before the addition of Ni. Compared with silicate sorption on $\gamma\text{-Al}_2\text{O}_3$ (Al–HSi), the added Ni competed with silicate for occupying the active sites of $\gamma\text{-Al}_2\text{O}_3$, which decreased the silicate sorption at $\gamma\text{-Al}_2\text{O}_3$ /water interfaces. The soluble Ni–Si complexes may also

influence silicate sorption. After the addition of Ni, silicate sorption proceeded in parallel with Ni sorption, indicating that the sorption of silicate occurred during Ni sorption on $\gamma\text{-Al}_2\text{O}_3$. For Al–LSiNi, silicate sorption mimicked the sorption curve of silicate in the Al–HSiNi system. The results indicated that the presence of silicate accumulated on the surface of $\gamma\text{-Al}_2\text{O}_3$. Small amounts of adsorbed silicate suggested weak sorption, rather than Ni–Si (co)precipitate formation. The uptake of silicate onto $\gamma\text{-Al}_2\text{O}_3$ occurred before Ni addition. The sequestration of silicate continued during the processes of Ni precipitation after Ni addition suggested that silicate may affect Ni sorption and the growth of Ni precipitates.

The results of Ni sorption on aluminum oxide^{1,25} and gibbsite²⁶ had demonstrated the formation of Ni–Al LDH precipitates. The formation of Ni phyllosilicate on a gibbsite–silica mixture, talc, silica, and montmorillonite had also been reported.^{3,9,10,27} Depège et al.²⁸ suggested the polymerization of silicates in LDH using either a coprecipitation method or an anionic exchange reaction. It is obvious that whether the silicate was dissolved from the sorbent or was added into the solution, they affected the formation of precipitates and their stability obviously. Further insight into the mechanism of silicate on Ni sorption and its precipitate formation were obtained by EXAFS spectra analysis in the following section.

EXAFS Spectra Analysis. *Influence of Silicate on the Formation of Ni–Al LDH.* Discrimination of the Ni–Al LDH or the Ni phyllosilicate phases requires the detection of Al atoms at a bond distance of 3.08 Å, which is about the same as that of Ni, or Si atoms at a bond distance of 3.26 Å.¹⁰ Scheinost et al.²⁶ and Manceau²⁹ employed ab initio FEFF calculations to investigate the influence of the weak backscatters of Si and Al on the Ni edge EXAFS (Figure S2), and they found that Al-for-Ni substitution dampened the second shell amplitude, whereas the presence of Si at the longer bond distance of 3.24–3.29 Å enhanced the second shell amplitude. Consequently, the fitted $\text{CN}_{\text{Ni-Ni}}$ below the crystallographic value of 6 for the second shell indicated the presence of the Al atom in the precipitate phase as Ni–Al LDH, whereas a $\text{CN}_{\text{Ni-Ni}}$ value above 6 indicated the presence of the Si atom in the precipitate phase as Ni phyllosilicate. Small clusters of Ni precipitates with a high percentage of octahedral at edge positions and with less than six neighbors, or the presence of additional outer-sphere adsorbed Ni without neighbors, may reduce the statistical coordination number or the second shell amplitude. The fitted $\text{CN}_{\text{Ni-Ni}}$ below/over the crystallographic value of 6 for the second shell was the coarse discrimination of the Ni–Al LDH or the Ni phyllosilicate phases. The method could not confirm the formation or the transformation of silicated Ni–Al LDH. The effects of Al or Si atoms in the Ni octahedral sheet were also found in the k^3 -weighted EXAFS spectra of reference samples. For Ni–Al LDH, the EXAFS spectrum has a distinctive beat pattern between 8.0 and 8.5 Å⁻¹, which can be used as a fingerprint to unequivocally identify the Ni–Al LDH precipitates.³⁰ Whereas Ni phyllosilicate, silicated Ni–Al LDH, and Ni(OH)₂ showed an elongated upward oscillation ending in a sharp tip at ca. 8.5 Å⁻¹, this oscillation seemed to be truncated for Ni–Al LDH (Figure S3, Table S1).¹⁰ The UV–vis diffuse reflectance spectra (DRS) can favorably complement the short-range order determinations by EXAFS.²⁶ Comparison with Ni model compounds showed that the ν_2 band at 15300 cm⁻¹ was a unique fingerprint of Ni–Al LDH,^{7,26} and the ν_2 band at 14900 cm⁻¹ was a unique fingerprint of $\alpha\text{-Ni}(\text{OH})_2$ (Figure S4, Table S2). High-resolution thermogravimetric

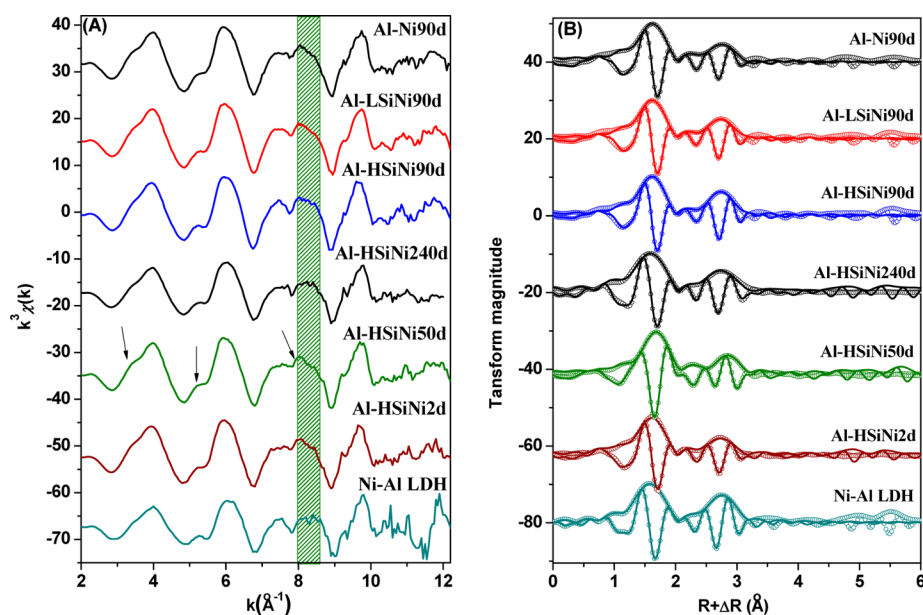


Figure 2. Raw k^3 -weighted $\chi(k)$ spectra of sorption samples and Ni–Al LDH reference sample (A) and their corresponding radial structure functions (RSFs) (B) (magnitude and imaginary part, symbols; fitted data, solid lines). The arrow indicated the appearance of a distinct feature at ~ 3.7 , ~ 5.1 , and $\sim 8.0 \text{ \AA}^{-1}$.

Table 1. Structure Parameters of Ni Adsorbed on $\gamma\text{-Al}_2\text{O}_3$ and Reference Ni–Al LDH (Ni/Al = 3) Sample^a

	first shell			second shell						
	Ni–O			Ni–Ni			Ni–Al			R_f
	R (Å)	CN	σ^2	R (Å)	CN	σ^2	R (Å)	CN	σ^2	
Al–Ni90d	2.05	5.7	0.0056	3.07	3.4	0.0088	3.07	2.5	0.009	0.67
Al–LSiNi90d	2.04	5.9	0.0062	3.08	4.3	0.0085	3.08	1.0	0.007	0.51
Al–HSiNi90d	2.05	5.8	0.0059	3.08	5.0	0.0069	3.08	0.9	0.009	0.33
Al–HSiNi240d	2.05	5.5	0.0049	3.08	5.1	0.0054	3.08	1.0	0.011	0.63
Al–HSiNi50d	2.05	5.4	0.0053	3.08	4.7	0.0061	3.08	0.8	0.010	0.56
Al–HSiNi2d	2.05	5.4	0.0055	3.08	4.3	0.0057	3.08	0.5	0.008	0.70
Ni–Al LDH	2.04	5.7	0.0042	3.08	4.1	0.0059	3.08	1.6	0.009	0.35

^aSingle and multishell fits carried out in R-space. CN: coordination number, R : interatomic distance, σ^2 : Debye–Waller factor, R_f : residual error in R space.

analysis (HRTGA) was successfully employed to show that a Ni–Al LDH transformed into a Ni–Al phyllosilicate precursor (Figure S5).⁷ With additional information obtained from the results of DRS, HRTGA, and wavelet analysis, we could distinguish whether Ni(OH)₂, Ni–Al LDH, or Ni phyllosilicate was formed in the samples.

Figure 2 showed the normalized, background-subtracted k^3 -weighted EXAFS spectra and their corresponding radial structure functions (RSFs) of Al–HSiNi, Al–LSiNi, and Al–Ni samples. The cutoff beat at $8.0\text{--}8.5 \text{ \AA}^{-1}$ was recognizable for the sorption samples, which identified the formation of Ni precipitates on $\gamma\text{-Al}_2\text{O}_3$ as the Ni–Al LDH phase in spite of the existence of silicate. The peak at $(R+\Delta R) \sim 2.75 \text{ \AA}$ may be attributed to the presence of Ni–Ni, Ni–Al, or Ni–Si bonds. The assumption of a Ni–Si contribution in the numerical simulation yielded poor fitting and a high R_f value. The accumulation of Ni–Ni and Ni–Al paths at the second shell and the fitting results suggested that no Ni–Si bond contributed to the formation of precipitates in Al–HSiNi and Al–LSiNi samples. The inability to fit Ni–Si in the octahedral layer was a proof of the absence of Ni phyllosilicate. The EXAFS spectra parameters (Table 1) indicated that the

presence of silicate affected the Ni bonding environment obviously, which were caused by variable relative amounts of Ni in Ni–Al LDH or the differences of Ni:Al ratios in the Ni–Al LDH crystallites.^{24,29}

The second peak was due to the contribution from the second nearest Ni and Al neighbors around the central Ni atom. From Table 1, one can see that Ni was surrounded by ~ 6 O atoms at $R_{\text{Ni–O}} = 2.04\text{--}2.05 \text{ \AA}$ in the first coordination shell. These results were similar to those previously reported for Ni species and were consistent with the NiO₆ octahedron.^{9,30} The results of EXAFS analyses suggested that the interatomic distance of Ni–Al ($R_{\text{Ni–Al}} = 3.08 \text{ \AA}$) was compatible with that of synthetic and natural Ni–Al LDH phases ($3.03\text{--}3.12 \text{ \AA}$).^{8,10} The microstructure of the Al–Ni sample was similar to those of Ni–Al LDH derived from Ni sorption on $\gamma\text{-Al}_2\text{O}_3$.¹ The amplitude of a second peak in the RSFs increased with increasing silicate concentration, which demonstrated that the presence of silicate increased the coordination number of Ni in Ni–Al LDH. The results suggested that the differences of Ni bonding environments were related to the Ni:Al ratio changes for the role of silicate. The fitting results of the second coordination shell showed that the number of second neighbor

Ni atoms (CN_{Ni-Ni}) at $R_{Ni-Ni} \sim 3.08 \text{ \AA}$ increased from 3.4 to 5.0, which was in good agreement with the stoichiometric change of Ni–Al LDH precipitates. The Ni–Al LDH was formed by the (co)precipitation processes of Ni and Al. In the presence of silicate, the DRS results (Figure S4) suggested that the Ni precipitate in the early stage should be α -Ni hydroxide without Al because of the insufficient amount of Al species in the aqueous solution, and then it would be progressively converted to Ni–Al LDH by the Al-for-Ni substitution because of the dissociation of Al from the γ - Al_2O_3 .^{24,26} The dissolution of Al for γ - Al_2O_3 and the actual concentration of Al for Al–HSi (Figure S6A) showed the inhabitation of the silicate for Al release. In the Al–Ni system (Figure S6B), the concentrations of Al in aqueous solution decreased with increasing reaction time as follows: 621.8 $\mu\text{g/L}$ (1 h), 168.6 $\mu\text{g/L}$ (5 h), and 16.3 $\mu\text{g/L}$ (12 h). For the Al–HSiNi system, the concentration of Al was lowered to 18.5 $\mu\text{g/L}$ after 1 h of contact time and then maintained the low concentration with increasing contact time. The dissociation rates of Al from γ - Al_2O_3 in the two systems can explain the difference in the stoichiometry of Ni–Al LDH. The surface coating of silicate on γ - Al_2O_3 reduced Al dissolution, the composition of Al in the Ni–Al LDH decreased, which resulted in the increasing of CN_{Ni-Ni} . The difference of Ni:Al ratios in the three aforementioned Ni–Al LDH samples was small, but noticeable, which may greatly influence the Ni–Al LDH stability. One could notice that the Ni:Al ratio of the synthetic LDH phase was lower than those of the Ni–Al LDH surface precipitates based on the $CN_{(Ni-Ni)}/CN_{(Ni-Al)}$, but the Ni–Al LDH actually had a significantly higher intensity for the Ni–Ni/Al shell in EXAFS Fourier transform (Figure 2). So, the Ni:Al ratio may not be the only determining factor for the higher Ni–Ni/Al shell. In addition, the particle size and/or crystallinity of the Ni–Al LDH could also affect the intensity of the Ni–Al/Ni shell. The presence of silicate could increase the particle size/crystallinity as silicate was a better interlayer anion than nitrate in compensating the positive charge of Ni–Al LDH.

Insight on the relationship between silicate and the Ni–Al LDH also needed to consider silicate uptake on solid phase after the addition of Ni. Because no Ni–Si bond was found in the EXAFS spectra of the sorption samples, the sorption of the silicate on the LDH precipitate or the (co)precipitation of silicate with Ni could be negligible. However, the possibility of the silicate sorption on the γ - Al_2O_3 surface or the exchange of silicate with NO_3^- in the interlayers of the precipitates was not excluded. The EXAFS technique was not able to discriminate the surface adsorbed silicate on γ - Al_2O_3 and the exchanged ones in the precipitates. For the Al–HSiNi system (Figure S7), high ionic strength decreased the silicate uptake, which suggested that silicate could replace NO_3^- in the precipitate interlayer. HRTGA was employed to characterize the intercalated silicates and the adsorbed ones. The data from the HRTGA experiments (Figure S5) demonstrated that Ni sorption on γ - Al_2O_3 in the presence of silicate resulted initially in the formation of α -Ni(OH)₂ precipitates followed by Al-for-Ni substitution and with time the subsequent conversion to a Ni–Al LDH. However, the transformation to silicated Ni–Al LDH or Ni phyllosilicate was not observed due to the small quantity of SiO_4^{2-} in the interlayer that could not result in the solid-state transformation of the precipitation phase (silication of Ni–Al LDH). The transformation of Ni phyllosilicate may take place at higher silicate concentration or need enough silicate supplements as Si-containing sorbents.

Effect of Aging Time on Ni Precipitates at γ - Al_2O_3 Surfaces in the Al–HSiNi System. As the reaction time increased from 2 to 240 days, the amounts of Ni on the mixture surface increased, leading to a more pronounced second shell as the reaction time continued (Figure 2). The growth of the second peak over aging time indicated that the formation of Ni–Al LDH was an important mechanism, which dominated Ni uptake after long reaction time.

The k^3 -weighted EXAFS spectra of the Al–HSiNi samples (Figure 2A) revealed the same feature of spectral details as the Ni–Al LDH reference, i.e., the weak splitting at 3.7 \AA^{-1} , the shoulder at 5.1 \AA^{-1} , and the beat pattern at 8.0 \AA^{-1} .⁶ Neither α -Ni(OH)₂ nor phyllosilicate-type precipitate was detected in all Al–HSiNi samples. Due to the higher thermodynamic stability of Ni–Al LDH, the transformation of Ni in α -Ni(OH)₂ into Ni–Al LDH as soon as Al species were available.²⁶ The fact that the dissolution of Al was suppressed by silicate, lower levels of Al species would result in a lower extent of Al substitution into the precipitates. The presence of silicate can exchange with NO_3^- in the interlayer of Ni–Al LDH and converts to a more stable precipitates with aging time continuing.^{3,27} This transformation could also lead to more stable surface precipitates as Ni phyllosilicate;²⁵ however, such phenomenon was not observed in our study. The facile formation of Ni phyllosilicate may be relative to the structures of Si-containing sorbents.^{3,9,10,27} Depège et al.²⁸ obtained the LDH phase containing silicate anions. However, the total concentration of silicate (0.08 M) was 160-fold higher than that of silicate (0.5 mM) in this study, which was an important factor that contributed to the transformation of LDH into a Ni phyllosilicate.

The structural parameters obtained by EXAFS analyses are summarized in Table 1. The EXAFS analyses suggested that Ni was surrounded by 6 O atoms in the first coordination shell, indicating that Ni located in an octahedral environment. The Ni–O bond distance ($R_{Ni-O} = 2.05 \text{ \AA}$) and CN values in the first shell were not affected by the aging time (Figure 2B). The R_{Ni-Ni} (3.08 \AA) was invariable, but CN_{Ni-Ni} increased from 4.3 to 5.1 as the reaction time increased from 2 to 240 days (Table 1), which suggested the nucleation and growth of a Ni–Al LDH.²⁵ Also, the Ni depletion from solution still slowed down slowly, and the dissolution of Al species from γ - Al_2O_3 still occurred. The continuous formation of Ni–Al LDH resulted in the increasing of CN_{Ni-Al} in the second coordination shell. The observation implied an amount of Al mass transfer from γ -alumina to the Ni–Al LDH, which could be an important mechanism for Ni–Al LDH formation. The Ni:Al ratio, calculated from the CN_{Ni-Ni}/CN_{Ni-Al} , decreased from 8.6 to 5.1 as the aging time increased from 2 to 240 d, due to the increasing particle size/crystallinity of the Ni–Al LDH. The time-variant feature of spectra was similar to earlier reports in which slow metal uptake was attributed to surface precipitates and/or nucleation processes after hours to months.^{10,25} The influence of silicate on the formation of Ni–Al LDH may affect the stability of the precipitation that would be addressed in the Dissolution section.

Influence of Addition Sequences on the Formation of Ni–Al LDH. In real environment, interferences from silicate can occur simultaneously with Ni sorption or after. The addition sequences influenced Ni sorption in batch experiments (Figure S1). Accordingly, the processes of Ni–Al LDH formation at solid surfaces may be different.

EXAFS spectra for the Al–HSiNi system prepared with different addition sequences are shown in Figure 3. The k^3 -

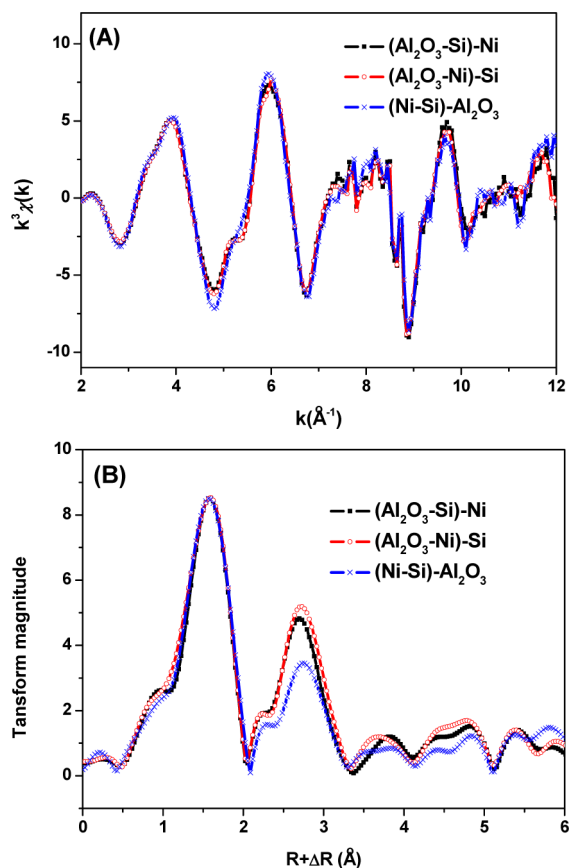


Figure 3. Influence of addition sequences for Al–HSiNi samples. k^3 -weighted $\chi(k)$ spectra (A) and corresponding radial structure functions (RSFs) (B).

weighted EXAFS spectra of these three samples were similar to that of Ni–Al LDH reference. The changes in spectral shape and frequency indicated that the coordination chemistry of Ni was different. The EXAFS spectra parameters (Table S3) indicated that the presence of silicate affected Ni bonding environment obviously. As mentioned above, one can draw the conclusion that silicate mainly influences the dissolution of Al for the transformation to Ni–Al LDH and/or the growth of Ni–Al LDH.^{4,25}

The sorption of Ni(II) in the $(\text{Al}_2\text{O}_3\text{--Ni})\text{--Si}$ system was similar to that of Ni(II) in the binary Al–Ni system. The subsequently added silicate may influence the growth/crystallinity of the Ni–Al LDH, while the pre-equilibrated 24 h or more without silicate greatly influenced the Ni:Al ratio for the Ni–Al LDH. For the $(\text{Al}_2\text{O}_3\text{--Si})\text{--Ni}$ system, the preretained silicate could decrease the dissociation of Al from $\gamma\text{-Al}_2\text{O}_3$ and accordingly decreased Al content in the Ni–Al LDH, which resulted in the higher $\text{CN}_{\text{Ni--Ni}}/\text{CN}_{\text{Ni--Al}}$ than the $(\text{Al}_2\text{O}_3\text{--Ni})\text{--Si}$ system. In the $(\text{Ni--Si})\text{--Al}_2\text{O}_3$ system, the Ni-silicate aqueous complexes interacted with $\gamma\text{-Al}_2\text{O}_3$, and the presence of silicate led to the formation of very poor crystallized Ni–Al LDH. Small or defected clusters of Ni–Al LDH with a high percentage of octahedral at edge positions resulted in the lower second shell amplitude.²⁶ One may speculate that this difference of finding is real and results from a difference in reaction conditions. The present study implied

that different addition sequences influenced the formation and crystallization of Ni–Al LDH, which was important for the understanding of the role of silicate in the Ni–Al LDH formation.

Dissolution. It must be addressed that the presence of silicate not only influenced Ni uptake and Ni:Al ratio in Ni–Al LDH but also played an important role in the stability of Ni–Al LDH. The dissolution of Ni–Al LDH was tested using HNO_3 at pH 4.0. The dissociation data of Ni from Al–HSiNi, Al–LSiNi, and Al–Ni were presented in Figure 4 as the relative amount of Ni remained on solid particles.

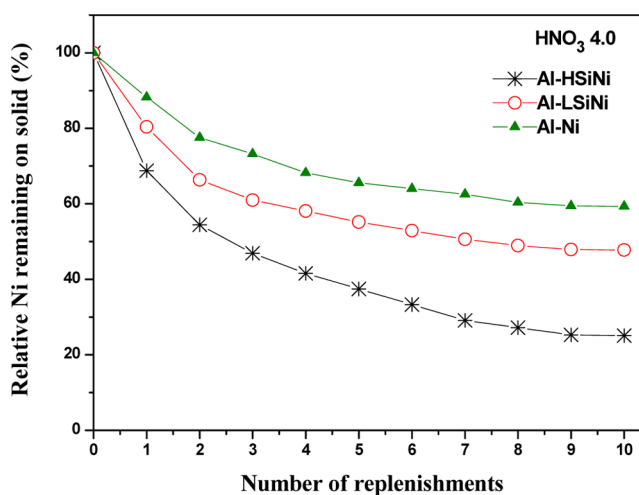


Figure 4. Macroscopic dissolution behavior of aged Ni precipitates on $\gamma\text{-Al}_2\text{O}_3$ showing the relative amount of Ni remaining on the surface following extraction with HNO_3 at pH 4.0 plotted against the total number of replenishments.

The proton-promoted dissolution was effective and a much larger fraction of Ni(II) was released from the surfaces. Similar release curves were previously reported for Ni precipitate on gibbsite,³ the difference between the extents of Ni–Al LDH resistance to proton-promoted was relative to the reaction conditions. Peltier et al.²⁴ reported that the extent of Ni–Al LDH resistance to dissolution was strongly substrate dependent. The structural difference between $\gamma\text{-Al}_2\text{O}_3$ and gibbsite may result in the formation of Ni precipitates with different stability. Surface protonation tended to be fast and resulted in polarization of the lattice sites around the metal center. Breaking of the metal–oxygen bond leading to detachment of the aqueous metal species was the rate-determining step.³¹ The presence of silicate could also affect the stability of the sorbent surface and mineral dissolution.³² The rate of Ni dissolution followed the sequences of Al–HSiNi > Al–LSiNi > Al–Ni. The dissolution results suggested that the silicate played important role in determining the stability of Ni–Al LDH. HNO_3 could remove Ni from a precipitate phase by proton dissolution, which was especially effective for a less stable Ni–Al LDH. Ni detachment was initially rapid at pH 4.0, which was attributable to the desorption of specifically adsorbed, mononuclear Ni ions.³ The dissolution rate then slowed down due to the gradual dissolution of Ni–Al LDH.^{3,6,7}

The presence of silicate may nevertheless affect the nature of Ni–Al LDH, especially the surface adsorbed silicate could affect the composition and stability of Ni–Al LDH.^{4,28} The dissociation rate of Al species from silicate coated $\gamma\text{-Al}_2\text{O}_3$ was relatively slow. Initial formed Ni–Al LDH could

incorporate with the dissolved Al species. With the addition of silicate, the lower levels of available Al species would result in a lower extent of Al substitution into the octahedral layers. The high susceptibility of Ni–Al LDH to dissolution may be due to the low Al substitution rates.⁶ The typical Ni:Al ratio in Ni–Al LDH is 2–4 with the Al substitution range of 20–33%.²⁴ Brindley³³ suggested that if Al substitution was below 20%, the homogeneous structure of the cation sheets began to break down, with isolated Al deficient regions to form nuclei of atoms, which resembled α -Ni(OH)₂ and thus could increase the overall solubility of the precipitate. The stability of the resulting Ni–Al LDH precipitate was one factor that may ascribe to Al release. However, the impact of silicate on Ni–Al LDH may contribute greatly to the dissolution. The (co)-precipitation of Ni and Al in the presence of silicate led to a very poorly crystallized Ni–Al LDH, which susceptibility to dissolution due to silicate prevented the crystallization of Ni–Al LDH.^{4,26} The stability of the Ni–Al LDH could be increased by exchange of silicate for NO₃³⁻. The effect of SiO₄²⁻-for-NO₃⁻ exchange was negligible due to the small quantity of SiO₄²⁻ in the interlayer that could not result in the solid-state transformation of the precipitation phase (silication of Ni–Al LDH). Other factors such as sorbent phase or precursor formation may also affect the formation and the stability of Ni precipitates.

Sequestration Mechanisms and Environmental Significance. Formation of Ni–Al LDH was an important mechanism of Ni retention in the silicate coated γ -Al₂O₃ system, α -Ni(OH)₂ was formed during the initial stage, and the formed α -Ni(OH)₂ could be converted into Ni–Al LDH by reaction with Al species in solution. The presence of the silicate was related to the initial formation of Ni precipitate nucleation and crystal growth. The surface adsorbed silicate on γ -Al₂O₃ occupied the active sites, which decreased the sorbent available surface area and selectivity for Ni and, consequently, decreased the growth of the nucleated Ni phase at the γ -Al₂O₃/water interface. The coated layer of silicate on the γ -Al₂O₃ surface had a significant negative effect on the Al dissolution rate. Then the substitution of Al into the octahedral layers of Ni–Al LDH decreased. The low Al-for-Ni substitution and the growth of Ni–Al LDH reduced their stability.⁴ Some silicate may insert into the interlayer of Ni–Al LDH. However, it could not make Ni–Al LDH transform to a more stable silicated Ni–Al LDH phase. Thus, although the formation of Ni–Al LDH can reduce Ni far below the level achieved by sorption, the chemical composition and the stability of Ni–Al LDH varied greatly depending on the concentration of silicate.

The presence of silicate influenced the formation and the speciation of the Ni–Al LDH. Silicate could suppress the amount of dissolved Al and resulted in less stable Ni–Al LDH with a high Ni:Al ratio. The Ni:Al ratios in the Ni–Al LDH decreased as the aging time increased. In summary, the formation of Ni–Al LDH in the natural environment would be less resistant to acid dissolution and may be longer-lasting with longer aging time. The stable Ni–Al LDH formation would occur more slowly with increased silicate content. These phenomena need to be considered in risk assessment and reactive transport modeling. The present study has great implications regarding the factors affecting the transfer and retention of metal ions in natural systems and should therefore require attention in the natural environment.

■ ASSOCIATED CONTENT

§ Supporting Information

Structure parameters of reference samples. Different addition sequences for Al–HSiNi systems. The different addition sequences on Ni uptake as a function of contact time for Al–HSiNi systems. FEFF simulations to investigate the influence of the weak backscatters Si and Al on the Ni edge XAFS. EXAFS of Ni reference Ni–Al LDH, silicated Ni–Al LDH, Ni phyllosilicate, β -Ni(OH)₂(s) and silicated β -Ni(OH)₂(s), and the Al–5mMSiNi30d sorption sample. DRS and HRTGA analysis for the conversion of α -Ni(OH)₂ to Ni–Al LDH with aging. The actual concentrations of Al for sorption systems. Silicate sorption kinetics at different ionic strength. This material is available free of charge via the Internet at <http://pubs.acs.org>.

■ AUTHOR INFORMATION

Corresponding Author

*Phone: +86-551-65592788. Fax: +86-551-65591310. E-mail: xkwang@ipp.ac.cn or xkwang@ncepu.edu.cn.

Notes

The authors declare no competing financial interest.

■ ACKNOWLEDGMENTS

The authors gratefully acknowledge the financial support from the National Natural Science Foundation of China (21377132, 41273134, 21307135, 21225730, 91326202), Hefei Center for Physical Science and Technology (2012FXZY005), and Jiangsu Provincial Key Laboratory of Radiation Medicine and Protection and the Priority Academic Program Development of Jiangsu Higher Education Institutions. We thank the staff of SSRF for their helpful technical assistance in the EXAFS data collection.

■ REFERENCES

- (1) d'Espinose de la Caillerie, J. B.; Kermarec, M.; Clause, O. Impregnation of γ -alumina with Ni(II) or Co(II) ions at neutral pH: hydrotalcite-type coprecipitate formation and characterization. *J. Am. Chem. Soc.* **1995**, *117*, 11471–11481.
- (2) McNear, D. H., Jr.; Chaney, R. L.; Sparks, D. L. The effect of soil type and chemical treatment on nickel speciation in refinery enriched soils: a multi-technique investigation. *Geochim. Cosmochim. Acta* **2007**, *71*, 2190–2208.
- (3) Scheckel, K. G.; Sparks, D. L. Dissolution kinetics of nickel surface precipitates on clay mineral and oxide surfaces. *Soil Sci. Soc. Am. J.* **2001**, *65*, 685–694.
- (4) Li, W.; Livi, K. J. T.; Xu, W.; Siebecker, M. G.; Wang, Y.; Phillips, B. L.; Sparks, D. L. Formation of crystalline Zn–Al layered double hydroxide precipitates on γ -alumina: the role of mineral dissolution. *Environ. Sci. Technol.* **2012**, *46*, 11670–11677.
- (5) Regelink, I. C.; Temminghoff, E. J. M. Ni adsorption and Ni–Al LDH precipitation in a sandy aquifer: an experimental and mechanistic modeling study. *Environ. Pollut.* **2011**, *159*, 716–721.
- (6) Voegeliin, A.; Kretzschmar, R. Formation and dissolution of single and mixed Zn and Ni precipitates in soil: evidence from column experiments and extended X-ray absorption fine structure spectroscopy. *Environ. Sci. Technol.* **2005**, *39*, 5311–5318.
- (7) Scheckel, K. G.; Scheinost, A. C.; Ford, R. G.; Sparks, D. L. Stability of layered Ni hydroxide surface precipitates—a dissolution kinetics study. *Geochim. Cosmochim. Acta* **2000**, *64*, 2727–2735.
- (8) Scheidegger, A. M.; Wieland, E.; Scheinost, A. C.; Dähn, R.; Spieler, P. Spectroscopic evidence for the formation of layered Ni–Al double hydroxides in cement. *Environ. Sci. Technol.* **2000**, *34*, 4545–4548.

- (9) Tan, X.; Hu, J.; Montavon, G.; Wang, X. Sorption speciation of nickel(II) onto Ca-montmorillonite: batch, EXAFS techniques and modeling. *Dalton Trans.* **2011**, *40*, 10953–10960.
- (10) Dähn, R.; Scheidegger, A. M.; Manceau, A.; Schlegel, M. L.; Baeyens, B.; Bradbury, M. H.; Morales, M. Neoformation of Ni phyllosilicate upon Ni uptake on montmorillonite: a kinetics study by powder and polarized extended X-ray absorption fine structure spectroscopy. *Geochim. Cosmochim. Acta* **2002**, *66*, 2335–2347.
- (11) Nachegeal, M.; Sparks, D. Nickel sequestration in a kaolinite-humic acid complex. *Environ. Sci. Technol.* **2003**, *37*, 529–534.
- (12) Yamaguchi, N. U.; Scheinost, A. C.; Sparks, D. L. Surface-induced nickel hydroxide precipitation in the presence of citrate and salicylate. *Soil Sci. Soc. Am. J.* **2001**, *65*, 729–736.
- (13) Naren, G.; Ohashi, H.; Okaue, Y.; Yokoyama, T. Adsorption kinetics of silicic acid on akaganeite. *J. Colloid Interface Sci.* **2013**, *399*, 87–91.
- (14) Song, Y.; Swedlund, P. J.; McIntosh, G. J.; Cowie, B. C. C.; Waterhouse, G. I. N.; Metson, J. B. The influence of surface structure on H₄SiO₄ oligomerization on rutile and amorphous TiO₂ surfaces: an ATR-IR and synchrotron XPS study. *Langmuir* **2012**, *28*, 16890–16899.
- (15) Hamid, R. D.; Swedlund, P. J.; Song, Y.; Miskelly, G. M. Ionic strength effects on silicic acid (H₄SiO₄) sorption and oligomerization on an iron oxide surface: an interesting interplay between electrostatic and chemical forces. *Langmuir* **2011**, *27*, 12930–12937.
- (16) Schlegel, M. L.; Manceau, A.; Charlet, L.; Chateigner, D.; Hazemann, J. L. Sorption of metal ions on clay minerals. III. Nucleation and epitaxial growth of Zn phyllosilicate on the edges of hectorite. *Geochim. Cosmochim. Acta* **2001**, *65*, 4155–4170.
- (17) Schlegel, M. L.; Manceau, A. Evidence for the nucleation and epitaxial growth of Zn phyllosilicate on montmorillonite. *Geochim. Cosmochim. Acta* **2006**, *70*, 901–917.
- (18) Chorover, J.; Choi, S.; Rotenberg, P.; Jeff Serne, R.; Rivera, N.; Strepka, C.; Thompson, A.; Mueller, K. T.; O'Day, P. A. Silicon control of strontium and cesium partitioning in hydroxide-weathered sediments. *Geochim. Cosmochim. Acta* **2008**, *72*, 2024–2047.
- (19) Waltham, C. A.; Eick, M. J. Kinetics of arsenic adsorption on goethite in the presence of sorbed silicic acid. *Soil Sci. Soc. Am. J.* **2002**, *66*, 818–825.
- (20) Seyfferth, A. L.; Fendorf, S. Silicate mineral impacts on the uptake and storage of arsenic and plant nutrients in rice (*Oryza sativa* L.). *Environ. Sci. Technol.* **2012**, *46*, 13176–13183.
- (21) Ford, R. G.; Scheinost, A. C.; Sparks, D. L. Frontiers in metal sorption/precipitation mechanisms on soil mineral surfaces. *Adv. Agron.* **2001**, *74*, 41–62.
- (22) Yang, S.; Sheng, G.; Montavon, G.; Guo, Z.; Tan, X.; Grambow, B.; Wang, X. Investigation of Eu(III) immobilization on γ -Al₂O₃ surfaces by combining batch technique and EXAFS analyses: role of contact time and humic acid. *Geochim. Cosmochim. Acta* **2013**, *121*, 84–104.
- (23) Rabung, Th.; Stumpf, Th.; Geckeis, H.; Klenze, R.; Kim, J. I. Sorption of Am(III) and Eu(III) onto γ -alumina: experiment and modeling. *Radiochim. Acta* **2000**, *88*, 711–716.
- (24) Peltier, E.; Lelie, D. V. D.; Sparks, D. Formation and stability of Ni-Al hydroxide phase in soils. *Environ. Sci. Technol.* **2010**, *44*, 302–308.
- (25) Scheidegger, A. M.; Strawn, D. G.; Lamble, G. M.; Sparks, D. L. The kinetics of mixed Ni-Al hydroxide formation on clay and aluminum oxide minerals: a time-resolved XAFS study. *Geochim. Cosmochim. Acta* **1998**, *62*, 2233–2245.
- (26) Scheinost, A. C.; Ford, R. G.; Sparks, D. L. The role of Al in the formation of secondary Ni precipitates on pyrophyllite, gibbsite, talc, and amorphous silica: a DRS study. *Geochim. Cosmochim. Acta* **1999**, *63*, 3193–3203.
- (27) Burattin, P.; Che, M.; Louis, C. Characterization of the Ni(II) phase formed on silica upon deposition-precipitation. *J. Phys. Chem. B* **1997**, *101*, 7060–7074.
- (28) Depège, C.; El Metoui, F. Z.; Forano, C.; de Roy, A.; Dupuis, J.; Besse, J. P. Polymerization of silicates in layered double hydroxides. *Chem. Mater.* **1996**, *8*, 952–960.
- (29) Manceau, A. Distribution of cations among the octahedral of phyllosilicates: insight from EXAFS. *Can. Mineral.* **1990**, *28*, 321–328.
- (30) Ren, X.; Yang, S.; Hu, F.; He, B.; Xu, J.; Tan, X.; Wang, X. Microscopic level investigation of Ni(II) sorption on Na-rectorite by EXAFS technique combined with statistical F-tests. *J. Hazard. Mater.* **2013**, *252–253*, 2–10.
- (31) Stumm, W.; Morgan, J. J. *Aquatic chemistry: Chemical equilibria and rates in natural waters*; Wiley: New York, 1996.
- (32) Scheckel, K. G.; Sparks, D. L. Kinetics of the formation and dissolution of Ni precipitates in a gibbsite/amorphous silica mixture. *J. Colloid Interface Sci.* **2000**, *229*, 222–229.
- (33) Brindley, G. W. Lattice parameters and compositional limits of mixed Mg, Al hydroxy structures. *Mineral. Mag.* **1980**, *43*, 1047–1047.